The Microphysics of Cosmic Ray transport

Alexandre Marcowith [1]
Alexandre.Marcowith@umontpellier.fr

[1] Laboratoire Univers et Particules de Montpellier
Université de Montpellier, IN2P3/CNRS

November 25, 2019

General outline

Two lectures ($\sim$ 40' each)

- Lecture 1: The physics of Cosmic Ray transport
- Lecture 2: The Astrophysics of Cosmic Ray transport

Lecture one : General outline

Lecture 1: The physics of Cosmic Ray transport

1. The different types of transport.
2. The wave-particle resonance process.
3. A (rapid) view on waves in the (single fluid) magnetohydrodynamic limit.
4. The quasi-linear theory of Cosmic Ray transport.
5. The drawbacks of the quasi-linear theory and some non-linear extensions.
6. Numerical simulations.
7. Perspectives.
8. Bibliography.

Outlines

From sub- to super-diffusion

We can characterize the transport regime using the root mean square (rms) displacement (in phase space)

$$\langle (x(t) - x(0))^2 \rangle^{1/2} = \langle \Delta x^2 \rangle^{1/2} \propto (\Delta t)^{\alpha}. \tag{1}$$

- $\alpha < 1/2$ sub-diffusion,
- $\alpha = 1/2$ diffusion or Brownian motion,
- $\alpha > 1/2$ super-diffusion, $\alpha = 1$ ballistic.

Here $\langle . \rangle$ is an appropriate averaging method of the sample of trajectories, usually over time and over several realizations of the sample.

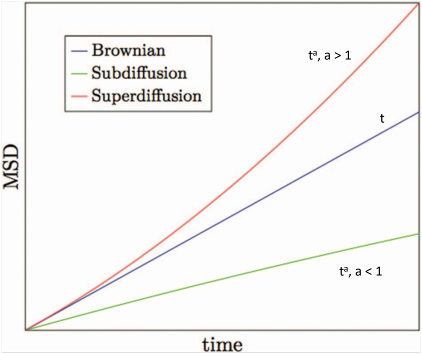

Illustration of the mean square displacement $\langle \Delta x \rangle^2$ as function of time for the three main transport regimes.

Outlines

A charged particle in an electro-magnetic field

The particle motion is controlled by the Lorentz force (in Gaussian CGS units) produced by the combined electric and magnetic effects.

$$\boxed{\frac{d\vec{p}}{dt} = q\left(\vec{E} + \frac{\vec{v}}{c} \wedge \vec{B}\right)} . \qquad (2)$$

where $\vec{p} = \gamma m\vec{v}$ is the particle momentum, with $\gamma = (1 - (v/c)^2)^{-1/2}$ is the particle Lorentz factor, q is its charge, m its mass.

- The magnetic field force does not produce any work but it induces a gyro (or Larmor) motion of the particle around the magnetic field direction.
- The electric force induces a variation of the particle energy.

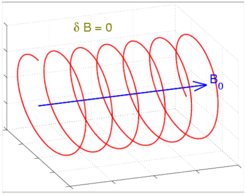

Larmor motion of a charged particle around an uniform magnetic field $\vec{B} = \vec{B}_0$.

The Larmor radius is:

$$\boxed{R_{\rm L} = \frac{v \sin\alpha}{\Omega_{\rm s}}} , \qquad (3)$$

- $\alpha = (\vec{v}, \vec{B})$ is the particle pitch-angle.
- $\Omega_{\rm s} = qB/\gamma mc$ is the synchrotron pulsation, the cyclotron pulsation is $\Omega_{\rm c} = qB/mc$.

Particle drifts

If we imposed another force (eg) perpendicular to the background magnetic field force then the centre of particle gyromotion has a drift. The Eq. of motion is (non-relativistic case)

$$m\frac{d\vec{v}}{dt} = q\frac{\vec{v}}{c} \wedge \vec{B} + \vec{F} \ , \tag{4}$$

The drift velocity imposed by the force $\vec{F}$ then reads:

$$\vec{v}_{\rm d} = c\frac{\vec{F} \wedge \vec{B}}{qB^2} \tag{5}$$

It is perpendicular to both $\vec{B}$ and $\vec{F}$. It can depend on the particle charge and mass (depending of the nature of the force $\vec{F}$).

See chapter 5 in B.V. Somov, Plasma Astrophysics, Springer.

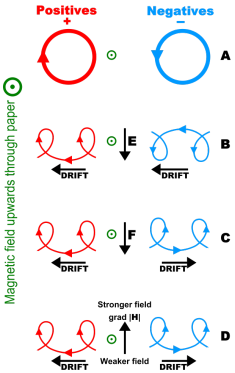

Particle drift produced by the electric force, another force (eg gravitational) and a gradient of the magnetic field, courtesy wikipedia.

Adiabatic invariants

A wave induces a local variation of the background magnetic fields [1] . On a more general aspect if the variation of the electromagnetic field occurs on scales L larger than $R_{\rm L}$ or on times T larger than the synchrotron/cyclotron pulsation $\Omega_{\rm s,c}^{-1}$ a series of quantities are conserved over the scales of variation.

1. Motion in the Larmor plane: the magnetic moment $\mathcal{M} = \frac{q\Omega_{\rm c}}{2\pi c}\pi R_{\rm L}^2$.
   $I_1 = \frac{\pi c}{e}\frac{p_\perp^2}{B} = \frac{2\pi mc}{e}\mathcal{M}$.
2. Longitudinal action invariant : $I_2 = p_{||}L$.
3. Conservation of the magnetic flux across the surface enclosed by the orbit of the guiding center motion: $I_3 = \int_S \vec{B}.d\vec{S} = \text{cst}$.

See chapter 6 in B.V. Somov, Plasma Astrophysics, Springer.

[1] background electric fields are usually screened because of the high conductivity of astrophysical plasmas

Mirroring/focusing effects

If the Larmor radius $R_L \ll L$, L the scale of variation of the magnetic field, then the first adiabatic invariant $p_\perp^2/B(z)$ is conserved over the particle trajectory. As no electric field is applied, the particle energy hence p^2 is conserved either. Hence we have:

$$\sin\alpha^2 = \sin\alpha_0^2 \frac{B}{B_0}\ ,\ \mathrm{B_0\ is\ the\ MF\ strength\ at\ the\ center\ of\ the\ mirror,} \qquad (6)$$

If we have the pitch-angle at the center $\alpha_0 < \alpha_{0m}$ such that $\sin\alpha_{0m} = 1/\sqrt{B_1/B_0}$ particles can escape the bottle. The angle α_{0m} is the loss cone.

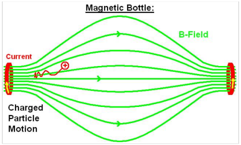

Particle trajectory in a magnetic bottle. B_0 and B_1 are the MF strengths at the center and at the edges.

This kind of (non-resonant) behavior is relevant for the propagation of low energy particles in long wavelength perturbations (or waves).

Resonant wave-particle interaction

The strongest interaction occurs when the Doppler-shifted wave pulsation in the frame moving parallel to the particle motion matches the synchrotron (or cyclotron) pulsation: Ω_s and its harmonics. Namely if,

$$\boxed{\omega(k) - k_{\parallel} v_{\parallel} = n\Omega_s} \ . \tag{7}$$

This is the Landau-synchrotron (or cyclotron) resonance condition.
$\omega(k)$ is the wave pulsation in the observer frame (see next for some particular types of waves), n is an integer, $v_{\parallel}$ is the particle speed along the MF, $k_{\parallel}$ is the wave number parallel to the MF.

1. $n \neq 0$ is the gyroresonance.
2. $n = 0$ is the Landau-Cherenkov or Cherenkov resonance. A mechanism associated with the linear Landau damping in unmagnetized media or with the transit-time damping process in magnetized media (see next).

Outlines

Magnetohydrodynamic approximation

Magnetohydrodynamics (MHD) is an approximate description of a plasma. It is valid in a restricted domain.
The MHD approximation is strictly valid if the collision time is the shortest, for long wavelengths and large times.

- **MHD is valid on long timescales**, timescales T longer than any characteristic plasma timescale. $T \gg (\Omega_c^{-1}, \omega_p^{-1})$.
  For an ion species of mass m_i we have $\Omega_{\rm c,i} \sim 9.6\ 10^3 Z(m_p/m_i) B_{\rm Gauss}$ rad/s. $B_{\rm Gauss}$ is the magnetic field in Gauss units. $\omega_p = \sqrt{4\pi n q^2/m}$ is the plasma pulsation for a plasma density n. For an ion species of mass m_i and density n_i we have $\omega_{p,i} = 1.3\ 10^3 Z\sqrt{(m_p/m_i) n_{i,\rm cc}}$ rad/s, m_p is the proton mass and $n_{i,\rm cc}$ is the ion density is units of $\rm cm^{-3}$.
- **MHD is valid on large lengthscales**, lengthscales L larger than the Debye length (the lengthscale beyond which the medium can be considered as quasi-neutral), $L \gg \lambda_{\rm D}$, with $\lambda_{\rm D} = \sqrt{k_{\rm B}T/4\pi n e^2} \simeq 7.4\ 10^2 \sqrt{T_{\rm eV}/n_{\rm cc}}$ cm. $T_{\rm eV}$ is the temperature in eV units.
  It also requires that $L \gg r_{\rm L}$, so its applicability domain fits with CR transport well because most of perturbations in the ISM verify this condition.

Equations of ideal magnetohydrodynamic (MHD)

1) Magnetized fluid equations:

Continuity equation: $\partial_t \rho + \vec{\nabla}.(\rho \vec{u}) = 0$

Momentum equation: $\left(\partial_t + \vec{u}.\vec{\nabla}\right)\vec{u} = \frac{\vec{J}\wedge\vec{B}}{\rho c} - \frac{1}{\rho}\vec{\nabla}P_{\rm g}$

Adiabatic energy equation: $\frac{d}{dt}\left(\frac{P_{\rm g}}{\rho^\gamma}\right) = 0$ (ignore thermal conduction, or non-adiabatic heating/cooling process, in that case we have to use an equation for internal energy)

2) Maxwell Equations:

Ampère's law: $\vec{J} = \frac{c}{4\pi}\vec{\nabla} \wedge \vec{B}$ (non-relativistic gas)

Faraday's law: $\partial_t B = -c\vec{\nabla} \wedge \vec{E}$

Divergence free law: $\vec{\nabla}.\vec{B} = 0$

Gauss's law: $\vec{\nabla}.\vec{E} = 4\pi \rho_{\rm c}$

3) Ideal Ohm's law:

$\vec{E} + \frac{\vec{u}}{c} \wedge \vec{B} = 0.$

More complete MHD models can be found in many different lectures (eg https://www.cfa.harvard.edu/~namurphy/Lectures/Ay253_2016_02_Ideal_MHD.pdf).

General relation dispersion of MHD waves

To obtain the MHD dispersion relation (giving $\omega(k)$) we must resolve the linearized system of the above MHD Eqs. Doing so (see the link above) we obtain [2]

$$\left(\omega^2 - k^2 u_A^2 \cos\theta^2\right)\left(\omega^4 - \omega^2 k^2 (u_A^2 + c_s^2) + k^4 u_A^2 c_s^2 \cos\theta^2\right) = 0\,. \quad (8)$$

θ is the wave pitch-angle (so $\cos(\theta) = \vec{k}.\vec{B}_0/kB_0$).

- $c_s = \sqrt{\gamma_{ad} k_B T/m}$ is the local ion (I assume proton) sound speed.
- $u_A = B/\sqrt{4\pi\rho}$ is the local Alfvén speed.

It can be decomposed into three type of waves:

1. (shear) Alfvén waves: $\omega_A = k_{||} u_A$. (they exist only in magnetized media)
2. Fast magnetosonic waves $\omega_F = k u_+$.
3. Slow magnetosonic (MS) waves $\omega_S = k u_-$.

with $u_\pm = \frac{1}{2}\left[u_A^2 + c_s^2 \pm \sqrt{(u_A^2 + c_s^2) - 4\, u_A^{\,2}\, c_s^{\,2}\ \cos^2\theta}\right]^{1/2}$.

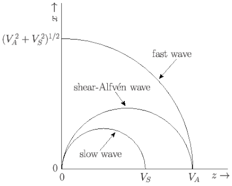

Phase speed of MHD dependence with the wave pitch-angle.

[2] Solving the linearized MHD Eqs leads to 7 modes: 2 Alfvén waves one forward one backward propagating, 2 fast modes, 2 slow modes and one entropy mode with $\omega = 0$.

Alfvén waves

Shear Alfvén waves

- Magnetic amplitude perturbations $\delta\vec{B}/B = -\delta\vec{u}/u_{\rm A}$.
- Perturbations perpendicular to the plane $(\vec{k},\vec{B})$, then $\delta\vec{B}.\vec{B} = \delta\vec{u}.\vec{B} = 0$. Transversal magnetic perturbations. So magnetic perturbations along the background MF vanish (at the lowest order).
- The electric perturbation $\delta\vec{E} \perp \delta\vec{B}$ and $\delta E = u_{\rm A}/c\delta B$.
- No density, pressure perturbations, $\delta\rho = \delta P = 0$.

Compressional Alfvén

- These waves have $\delta\vec{u}.\vec{B} \neq 0$
- Usually non-vanishing density and pressure perturbations.
- Dispersion relation $\omega = ku_{\rm A}$.

Magnetosonic waves

- We always have $u_- \leq u_{\rm A} \leq u_+$
- Combination of compressional and sound waves.
- Non vanishing density, pressure perturbations.
- Have also a magnetic perturbation component parrallel to $\vec{B}$. In general these waves have motions and perturbations parallel *and* perpendicular to $\vec{B}$, but $\delta\vec{E} \perp \vec{B}$.

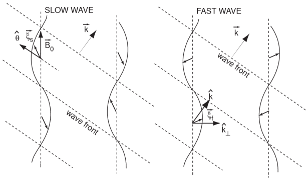

Slow and fast waves in real space (B-k plane). For the fast wave, for example, density (inferred by the directions of the displacement vectors ξ) becomes higher where field lines are closer, resulting in a strong restoring force, which is why fast waves are faster than slow waves. From Cho et al 2002.

Outlines

Gyroresonance

The condition for the resonance with Alfvén waves (the discussion is similar for MS waves) is

$$k_{\|} \left(u_{\rm A} - v_{\|}\right) = n\Omega_{\rm s} \tag{9}$$

Usually harmonics n=(1, -1) dominate the interaction, they are associated with wave polarization (+1 right-handed, -1 left-handed). Usually also, parallel particle speed are in far excess wrt to the Alfvén speed ($\sim$ 10 km/s in the ISM). So the condition for relativistic particles reads approximately:

$$k_{\|} R_{\rm g} \cos(\alpha) \sim \mp 1 \ , \tag{10}$$

where $R_{\rm g} = R_{\rm L}/\sin(\alpha)$ is the particle gyro-radius. So for particles propagating along the magnetic field we have $|kR_{\rm g}| \sim 1$ for resonant waves.

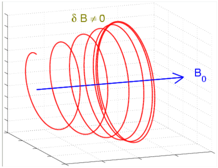

Perturbed gyromotion maximal at resonance for $kR_{\rm g} \sim 1$.

In the Lorentz Eq. the term $q\frac{\vec{v}}{c} \wedge \delta\vec{B}$ induces a scattering of the particle pitch ange α, this one becomes a random variable. The scattering effect is maximum when the wave-particle resonance condition is fulfilled.

Transit-time damping

Physically speaking the process involves the interaction between the particle magnetic moment $M = q\Omega_c/2\pi c(\pi R_g^2)$ with the magnetic gradient parallel to the background MF. (Magnetic analog to Landau damping.)

The transit-time damping occurs at the Cherenkov resonance for a MS wave,

$$\omega(k) = k u_{F/S} = k_{\parallel} v_{\parallel} \ . \quad (11)$$

Then,

$$v_{\parallel} = u_{F/S}/\cos(\theta) \ . \quad (12)$$

No scale appear in the resonant condition. The particle interacts only with the wave propagating in the same direction.

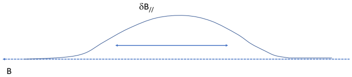

Transit-time damping Interaction of a particle with a perturbation with $\delta B_{\parallel} \neq 0$.

The physics of the parallel (wrt to the MF) transport

The parallel transport is due to the time variation of the particle pitch-angle cosine $\mu = \cos(\alpha)$. Consider for instance Alfvén perturbations we have, for $\vec{B} = B\vec{e}_{\rm z}$ (neglecting electric field effects)

$$\dot{\mu} = \frac{\Omega_{\rm s}}{v} \left(v_{\rm x} b_{\rm y} - v_{\rm y} b_{\rm x} \right) \ , \tag{13}$$

where $\vec{b} = \delta\vec{B}/B$. As μ becomes a random variable the particle undertakes a diffusion along $\vec{B}$. It is characterized by the cosine pitch-angle diffusion coefficient (accounts for the correlation of the variation of μ along time)

$$D_{\mu\mu}(\mu) = \int_0^{\infty} dt \langle \dot{\mu}(t)\dot{\mu}(0) \rangle \ . \tag{14}$$

We define the parallel diffusion coefficient as

$$\kappa_{\|} = \frac{v^2}{8} \int_{-1}^{1} d\mu \frac{(1-\mu^2)^2}{D_{\mu\mu}} \ . \tag{15}$$

The physics of the perpendicular transport

The perpendicular transport is associated with two processes.

- Pitch-angle scattering induces a jump from one field line to another. This is characterized by a diffusion coefficient $\kappa_\perp$ usually $\ll \kappa_\parallel$. (we assume $\delta B_\parallel = 0$), the perturbed Eq. of motion is $v_x = v_z b_x$. We define

$$\kappa_\perp = \kappa_{xx} = \int_0^\infty \langle v_x(t) v_x(0) \rangle dt \ . \tag{16}$$

A general formulation of the ratio $\kappa_\perp/\kappa_\parallel$ can be found in Chuvilgin & Ptuskin (1993)

$$\kappa_\perp = \kappa_\parallel \frac{\varepsilon^2}{1+\varepsilon}, \tag{17}$$

where $\varepsilon = \frac{\nu_s}{\Omega_s} < 1$.

- The magnetic field lines being turbulent, two close magnetic field lines at a position s=0 will diverge from each other as $s > 0$: magnetic field line wandering process. This is characterized by a magnetic diffusion coefficient κ_M. (see figure extracted from & Goldreich 2001).

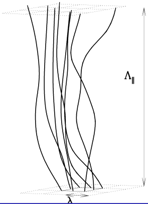

Outlines

Diffusion coefficient calculation

A simple mathematical formulation with a complex physical solution. Let us consider the evolution of the pitch-angle cosine. Using Eqs 13 and 14 we have

$$D_{\mu\mu} = \int_0^{\infty} dt \langle \dot{\mu}(t)\dot{\mu}(0)\rangle \propto \int_0^{\infty} dt \left(\langle v_{\rm x}(t) b_{\rm y}(t) v_{\rm y}(0) b_{\rm x}(0)\rangle + \ldots\right) \ .$$

The diffusion coefficient depends hence on a correlator of the fourth order, usually difficult to estimate analytically which depends on unknown quantities $\vec{x}(t)$ the particle position at different time (which themselves are deduced from the diffusion process).
One way to proceed is to consider that the particle trajectory in the above formulation is given by the particle unperturbed trajectory, ie in an unperturbed EM field. This is the so-called quasi-linear theory (henceforth QLT).
It is a first order perturbation theory, corresponding to the Born approximation in scattering theory (see Pelletier 1977).

Applicability domain of the QLT

There are two main conditions for the QLT to apply:

1. The perturbed fields need to have a small amplitude. Namely $\delta B/B, c\delta E/B \ll 1$.
2. The perturbed fields need to have components displayed over many scales. In other words we need to have a fully developed turbulence.

The theory is effectively applicable in a restricted domain of timescales: $t_{\rm c} \ll t \ll t_{\rm d}$, where $t_{\rm c}$ is the correlation time between stochastic forces and $t_{\rm d}$ is the timescale of the evolution of the mean particle distribution function.

For instance consider a turbulent spectrum $kW(k) = \delta B(k)^2$, if particle undergoes resonant interaction with modes k then $t_{\rm c} \sim \Omega_{\rm s}^{-1} k/\Delta k$, Δk is the spectrum width in the parallel MF direction (see §A in Casse et al 2002), while $t_{\rm s} \sim \Omega_{\rm s}^{-1} (B/\delta B)^2$. Hence $t_{\rm c} \ll t_{\rm d}$, gives $(\delta B/B)^2 \ll \Delta k/k$, so $\Delta k/k$ can not be too small.
Its applicability then depends on the turbulence model (W(k)), usually it is rather restricted but QLT is the main theory used in CR transport studies in Astrophysics.

How to describe magnetic turbulence?

In the diffusion coefficient calculation we have at some stage [3] to evaluate a two-point correlation tensor of turbulent fields (velocity, magnetic and electric fields). For the magnetic field terms like (i,j are running over x,y,z).

$$R_{ij}(\vec{x}, t, \vec{x}_0, t_0) = \langle \delta B_i(\vec{x}, t) \delta B_j^{cc}(\vec{x}_0, t_0) \rangle . \tag{18}$$

This can be evaluated by means of the Fourier transform of the magnetic fluctuations $\delta B_i(\vec{x}, t) = \int d^3\vec{k} \delta B_i(\vec{k}, t) \exp\left(i\vec{k}.\vec{x}\right)$. If we consider homogeneous (only dependent on the relative position) turbulence Eq.18 reads (taking $t_0 = 0$ and $\vec{x}_0 = \vec{0}$).

$$R_{ij}(\vec{x}, t) = \int d^3\vec{k} P_{ij}(\vec{k}, t) \exp\left(i\vec{k}.\vec{x}\right) , \tag{19}$$

where $P_{ij}(\vec{k}, t)\delta(\vec{k} - \vec{k}') = \langle \delta B_i(\vec{k}, t) \delta B_i(\vec{k}', 0) \rangle$ is the turbulent power spectrum:

$$P_{ij}(\vec{k}, t) = P_{ij}(\vec{k}, 0)\Gamma(\vec{k}, t) , \tag{20}$$

Γ is the dynamical function, it is set to 0 for magnetostatic turbulence.

[3] different hypothesis permit to reduce the fourth order correlation tensors in slide 25 to a product of second order correlation tensors. In the QLT framework $v_{\rm x}$ and $v_{\rm y}$ are given by the Larmor gyration. See eg Shalchi: Non-linear CR diffusion theories, Springer.

Magnetostatic slab turbulence

This model is somehow unrealistic and have some pathological defaults (see next) but it is educative. The magnetic tensor in slab turbulence is (§2.1.2 A. Shalchi Non linear Cosmic Ray diffusion theories Springer). Slab turbulence is composed of modes propagating in 1D direction parallel to the background MF.

$$P_{ij}(\vec{k}) = W(k_{||})\frac{\delta(k_\perp)}{k_\perp}\delta_{\rm ij}\ , \text{for i, j} = \text{(x, y)} \tag{21}$$

W(k) is the turbulent spectrum such that $\int W(k) d^3\vec{k} = \delta B^2/2$. Then, different models exist to express the wave number dependence of $W(k)$ we can for instance choose a Kolmogorov spectrum $W(k_{||}) \propto k_{||}^{-5/3}$.

QLT parallel CR mean free path in a simple case: slab-type turbulence

§3.2.1 in Shalchi book gives the $D_{\mu\mu}$ coefficient is slab turbulence. The procedure is as follows: 1) consider unperturbed Larmor gyromotion to infer particle position (QLT hypothesis) 2) express $\dot{\mu}$ in terms magnetic perturbation components only as the velocity components are known 3) derive the two-point correlation tensor 4) express $D_{\mu\mu}$ in terms of W(k).
We find

$$D_{\mu\mu} = \frac{2\pi v^2(1-\mu^2)}{B^2 R_{\rm L}^2} \int_0^\infty dk_{||} W(k_{||}) \left(R_1(k_{||}) + R_{-1}(k_{||})\right) \ . \quad (22)$$

$R_{\rm n}(k_{||})$ is the resonance function of order n, in the QLT it is $R_{\rm n}(k_{||}) \simeq \pi\delta(k_{||} v\mu + n\Omega_{\rm s})$. Using $W(k) = W_0(kL)^{-\alpha}$ ($k \equiv k_{||}$) we have:

$$D_{\mu\mu} \simeq \frac{\pi}{2}\frac{v}{L}\left(\frac{\delta B}{B}\right)^2 (\alpha-1)(1-\mu^2)\mu^{\alpha-1}R^{\alpha-2} \ , \quad (23)$$

L is the injection scale of the turbulence, $R = R_{\rm L}/L$. We have using Eq. 15

$$\kappa_{||} \simeq vL\left(\frac{B}{\delta B}\right)^2 R^{2-\alpha} G(\alpha) \ , \lambda_{||} = 3/v\kappa_{||} \ . \quad (24)$$

If $\alpha < 2$ the parallel mfp $\lambda_{||}$ is increasing with the energy (eg for Kolmogorov it scales as $E^{1/3}$) and scales as $(B/\delta B)^2$. ($G(\alpha)$ can be found in Shalchi book)).

QLT perpendicular CR mean free path in a simple case: slab-type turbulence

If we consider Alfvénic perturbation we have $\delta B_{||} = 0$ so the particle speed is (Shalchi §3.3.3)

$$v_x = v_{||} \frac{\delta B_x}{B} \tag{25}$$

Using Eq. 16 we have (the unperturbed parallel motion is $z(t) = v\mu t$)

$$\kappa_{xx} = \frac{v^2\mu^2}{B^2} \int_0^\infty dt \langle \delta B_x(z) \delta B_x(0) \rangle \simeq \frac{v|\mu|}{B^2} \int_0^\infty dz \langle \delta B_x(z) \delta B_x(0) \rangle \; . \tag{26}$$

It can be expressed in terms of the slab turbulence correlation length ℓ, with $\ell \delta B^2 = \int_0^\infty dz R_{xx}(z)$. We have the perpendicular diffusion coefficient and mfp:

$$\kappa_\perp = \kappa_{xx} \simeq \frac{v|\mu|}{2} \frac{\delta B^2}{B^2} \ell \, , \lambda_\perp = 3/v\kappa_\perp \simeq \frac{3}{4} \left(\frac{\delta B}{B} \right)^2 \ell \; . \tag{27}$$

Some important remarks:

- The perpendicular transport in slab magnetostatic turbulence is controlled by the field line wandering process.
- The ratio $\lambda_{||}/\lambda_\perp \propto \left(\frac{B}{\delta B}\right)^4$ so $\lambda_{||} \gg \lambda_\perp$.

Other types of magnetostatic turbulence models

The general form of axisymmetric turbulence (Matthaeus & Smith 1981, §2.1.2 Shalchi book)

$$P_{ij}(\vec{k}) = A(k_{\|}, k_{\perp}) \left(\delta_{\rm ij} - \frac{k_i k_j}{k^2} + i\sigma(k_{\|}, k_{\perp}) \sum_k \epsilon_{ijk} \frac{k_k}{k} \right) . \quad (28)$$

- The tensor σ is the magnetic helicity (the relative amount of forward and backward propagating perturbations along the MF).
- The function A describes the turbulence geometry (isotropic or not).
- Turbulence models then differ by their spectrum.

1. Slab type turbulence $A = W(k_{\|}) \frac{\delta(k_{\perp})}{k_{\perp}}$.
2. 2D model $A = W(k_{\perp}) \frac{\delta(k_{\|})}{k_{\perp}}$.
3. The composite model slab/2D. The solar wind turbulence at 1 AU can be roughly modeled by a composite model with 20% slab and 80% 2D (Bieber et al 1996).
4. Isotropic model $A(k)$.
5. The Goldreich-Sridhar model (see lecture 2) is anisotropic.

Outlines

QLT: main caveats

- The 90^o scattering problem. Just consider again the pitch-angle cosine diffusion coefficient in slab turbulence

$$D_{\mu\mu} \simeq \frac{\pi}{2}\frac{v}{L}\left(\frac{\delta B}{B}\right)^2 (\alpha - 1)(1-\mu^2)\mu^{\alpha-1}R^{\alpha-2}\,, \tag{29}$$

  As $\mu \to 0$ it may vanish if $\alpha > 1$, hence the parallel mfp $\lambda_{\|} \propto (1-\mu^2)^2/D_{\mu\mu}$ can diverge. This is the so-called 90^0 scattering problem.

- Perpendicular diffusion regimes. For instance slab turbulence analytical results find the particles undertakes a diffusion perpendicular to the mean MF (slide 30). In fact, simulations (see next) find a different behavior, namely a subdiffusion, $\langle \Delta x^2 \rangle \propto \sqrt{t}$ (Qin et al 2002). This can not be explained in the framework of QLT and requires more refined treatments. Discrepancies have been also found for other type of turbulence models.
- I should add that QLT is limited in a rather restricted timescale range.

Linear extension of the QLT: non magnetostatic models

The turbulent power spectrum given by Eq. 20 is in general time dependent, the function $\Gamma \neq 0$. This means that turbulent motions have a finite correlation time t_c. Several models have been adopted

- The damping model $\Gamma = \exp(-t/t_c)$ (see Bieber et al 1994).
- The random sweeping model $\Gamma = \exp -(t/t_c)^2$, this assumes that turbulent Eddies interact randomly (see Bieber et al 1994).
- Wave turbulence model $\Gamma = \exp(i\omega t - \gamma_d t)$, ω is the wave dispersion relation (eg for Alfvén waves $\omega = k_{||} u_A$), and γ_d is a wave damping process (eg Landau damping). (see Schlickeiser 2002).

If we assume this, the resonance function that appears in the calculation of diffusion coefficient (eg in Eq 22) is not a Dirac peak anymore. The resonance is broadened. For instance in the damping model the resonance function is expressed in terms of a Breit-Wigner function $R \sim t_c^{-1}/(t_c^{-2} + (v\mu k_{||} + n\Omega_s)^2)$.

Non-linear extensions of the QLT: resonance broadening

How to treat the 90^o scattering problem ? The calculation is due to Völk (1975) and is described in the Shalchi book.
If magnetic perturbation propagate along the mean MF it induces a variation of the magnetic field. If the lenthscale of the variation is larger than the CR Larmor radius then $p_\perp^2/B$ is conserved (see slide 11), so if p is also conserved (neglecting electrical effects) μ varies. So a resonance that would occur only at $\mu = 0$ is enlarged.
Völk (1975) evaluates the uncertainty in the parallel speed to be

$$\frac{\Delta v_\parallel}{v_\perp} \simeq \frac{(\delta B)^{1/2}}{\sqrt{B}} \ . \tag{30}$$

This produces a perturbation of the guiding center position with respect to its mean position $\langle z \rangle = v\mu t$. The resonance condition reads assuming a Gaussian distribution wrt to this position (Yan & Lazarian 2008)

$$R_n \simeq \frac{\sqrt{\pi}}{|k_\parallel \Delta v_\parallel|} \exp\left(-(k_\parallel v_\parallel + n\Omega_s)^2/k_\parallel^2 \Delta v_\parallel^2\right) \ . \tag{31}$$

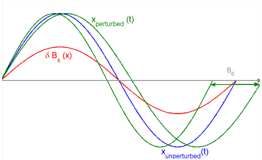

Perturbed trajectory due to a variation fo the magnetic field : resonance braodening

Non-linear extensions of the QLT: more complex modelling

These aspects are beyond the scope (the time constraints) of these lectures and are exposed in the Shalchi book (see §4-7, and references therein).

One idea is for instance to go to the second order in the perturbative theory (second order QLT), that is to retain as CR trajectories the updated positions obtained from the QLT and re-inject them into the diffusion coefficient calculations.

Other non-linear theories have been developed to evaluate the guiding-center motion, so to treat the perpendicular transport problem more adequately. This the case of the so-called extended non-linear guiding center theory. This accounts for the resonance broadening effects due to the variation of μ in a magnetic perturbation for the calculation of the perpendicular diffusion coefficient (but not only).

Outlines

Different techniques

CR propagation in synthetic turbulence models - test particle/test-wave simulations.
The turbulence is set in a simulation box with a prescribed model, eg slab, 2D, composite, isotropic, Goldreich-Sridhar. The turbulent perturbations are generated either using a set of plane waves (Giacalone & Jokipii 1999) or using Fast-Fourier transforms (Casse et al 2002).

CR propagation in MHD code-generated turbulence models - test particle simulations.
Particle are propagated in a series of MHD snapshots issued from a MHD simulations of a turbulent box (Xu & Yan 2013, Cohet & Marcowith 2016).

CR transport coupled to MHD solutions Particle transport effects are inserted into source terms of MHD Eqs (see slide 16) and then self-consistent calculations can be performed.
CR are either be treated as a supplementary fluid (Drury & Völk 1981, Ipavich 1975), so a supplementary energy equation is added or CR are treated using a kinetic Eq by the mean of a particle-in-cell technique (Bai et al 2015, van Marle 2018) or with the help of a Vlasov Eq (Reville & Bell 2012).

Synthetic turbulence simulations

The turbulence is generated using plane wave development (Batchelor 1960, Giacalone & Jokipii 1999).

$$\delta\vec{B}(x,y,z) = \sum_{i=1}^{N_m} A(k_n)\vec{\xi}_n \exp\left(i\, k_n z'_n + i\phi_n\right) \quad (32)$$

with $\vec{\xi}_n = \cos(\alpha_n)\vec{x}'_n + i\sin(\alpha_n)\vec{y}'_n$ is the polarization vector $A(k_n)$ is the wave amplitude $\propto \delta B^2$, β_n is a random phase.
The FFT method (Casse et al 2002) is similar except that the wavenumber vectors are defined over a grid.
Particles are then propagated in the magnetic turbulence solving the Lorentz Eq. using different methods : Runge-Kutta of high orders, Bulirsch-Stoer ... (see Press et al 1992).
The diffusion coefficients are reconstructed using a high number of particles (a few tens of thousand) to propagate in several magnetic turbulence realizations. E.g. calculating $z(t)$ the position of the particle wrt to the background MF, we have (for N_r realizations, N_p particles)

$$\kappa_{\parallel}(t) = \frac{\langle z^2(t) - z^2(0)\rangle}{2t} = \frac{1}{N_r}\frac{1}{N_p}\sum_{i=1}^{N_r}\sum_{j=1}^{N_p}\frac{(z_{ij}^2(t) - z_{ij}^2(0))}{2t}. \quad (33)$$

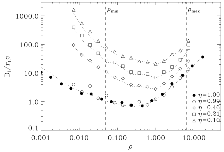

Synthetic simulations of the parallel diffusion coefficient in the case of isotropic Kolmogorov turbulence: full dots: plane wave method, empty dots: FFT, from Casse et al 2002

The unprimed coordinate system has the background magnetic field along the z-axis, and the primed coordinate system is obtained from the unprimed

MHD turbulence models

The particle trajectories are integrated using similar type of integration schemes, except that the magnetic field is calculated from a MHD code. Only a few works in Astrophysics among which Xu & Yan (2013), Cohet & AM (2016), see review by Mertsch (2019).

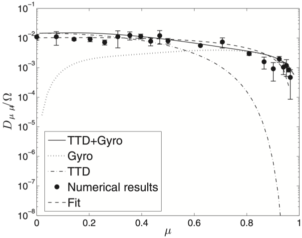

Calculation of the $D_{\mu\mu}$ coefficient at $R = 0.03$ for incompressible forcing a 512^3 box, $M_A = u_{turb}/u_A = 0.5$. From Xu & Yan (2013)

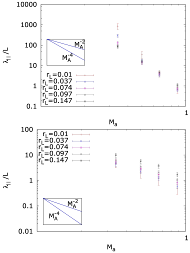

CR mfp for two different types of forcing up: incompressible forcing, down: compressible forcing as function of M_A. From Cohet & AM (2016).

Beyond particle-test and test-wave cases: the full coupling

Two methods to account for CR backreaction, one is fluid, one is kinetic (this can be split into two).

1. Bi-fluid method: It consists in adding an energy Eq. for CR energy density $e_{\rm CR}$.
2. Particle-in-cell in MHD method: it consists in adding a particle-in-cell module (a module solving the Lorentz Eq.) to the MHD code, BUT including CR backreaction through a modification of the Ohm's law to account for the electric field produced by the CR distribution. CR current is also included into the Lorentz force in the Euler/ energy fluid Eqs.
3. Vlasov-Fokker-Planck approach: it consists at solving a kinetic Eq. for CRs and then doing the same procedure as in the PIC-MHD simulations.

Outlines

Perspectives

- Rapid progresses in numerics, especially while dealing with CR back-reaction (multi-fluid, MHD-kinetic methods)
- But basic processes not fully understood yet. Wave-particle interaction is a complex problem involving non-linear effects (trapping ...).
- The exact level of magnetic fluctuations in the interstellar medium depends on many type of instabilities and processes. (As we will now see.)

Outlines

References

- X. Bai et al, 2015, ApJ, 809, 55. Magnetohydrodynamic-particle-in-cell Method for Coupling Cosmic Rays with a Thermal Plasma: Application to Non-relativistic Shocks.
- J.W. Bieber et al, 1994, ApJ, 420, 294. Proton and Electron Mean Free Paths: The Palmer Consensus Revisited.
- F. Casse, M. Lemoine, G. Pelletier, 2002, PhRvD, 65, 3002. Transport of cosmic rays in chaotic magnetic fields.
- R. Cohet & A. Marcowith, 2016, A&A, 588, 73. Cosmic ray propagation in sub-Alfvnic magnetohydrodynamic turbulence.
- J.Cho, A. Lazarian, E. Vishniac, 2002 ApJ, 564, 291. Simulations of Magnetohydrodynamic Turbulence in a Strongly Magnetized Medium.
- L.G. Chuvilgin & V.S. Ptuskin, 1993, A&A, 279, 278. Anomalous diffusion of cosmic rays across the magnetic field.
- L.O'C. Drury & H.J. Voelk, 1981, ApJ, 248, 344. Hydromagnetic shock structure in the presence of cosmic rays
- J. Giacalone & R. L. Jokipii, 1999, ApJ, 520, 204. The Transport of Cosmic Rays across a Turbulent Magnetic Field.
- F.M. Ipavich, 1975, ApJ, 196, 107. Galactic winds driven by cosmic rays.
- Y. Lithwick, P. Goldreich, 2001, ApJ, 562, 279. Compressible Magnetohydrodynamic Turbulence in Interstellar Plasmas.
- A.J. van Marle, F. Casse & A. Marcowith, 2018, MNRAS, 473, 3394. On magnetic field amplification and particle acceleration near non-relativistic astrophysical shocks: particles in MHD cells simulations.
- P. Mertsch, 2019, arXiv191001172.Test particle simulations of cosmic rays.
- G. Pelletier, 1977, JPlPh,18,49. Renormalization method and singularities in the theory of Langmuir turbulence.
- B. Reville & A.R. Bell, 2012, MNRAS, 419, 2433. A filamentation instability for streaming cosmic rays.
- H.J. Voelk, 1975, Cosmic ray propagation in interplanetary space, Reviews of Geophysics and Space Physics, 13, 547.
- S. Xu & H. Yan, 2013, ApJ, 779, 140. Cosmic-Ray Parallel and Perpendicular Transport in Turbulent Magnetic Fields.
- H. Yan & A. Lazarian, 2004, Cosmic-Ray Scattering and Streaming in Compressible Magnetohydrodynamic Turbulence, ApJ, 614, 757.
- H. Yan & A. Lazarian, 2008, Cosmic-Ray Propagation: Nonlinear Diffusion Parallel and Perpendicular to Mean Magnetic Field, ApJ, 673, 942.

Lecture two: General outline

Lecture 2: The Astrophysics of Cosmic Ray transport

1. The magnetohydrodynamic turbulence in the ISM.
2. Cosmic Ray Anisotropy and turbulence.
3. The different ISM phases and their impact over MHD turbulence and CR propagation.
4. Some recent modelling of CR transport: self-generated turbulence versus background turbulence.
5. The problem of propagation close to sources and CR halos.
6. Some perspectives.
7. Bibliography.

Outlines

The turbulent Milky-way

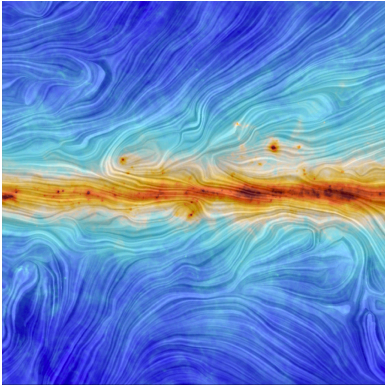

Planck satellite data: The color scale represents the total intensity of dust emission, revealing the structure of interstellar clouds in the Milky Way. The texture is based on measurements of the direction of the polarized light emitted by the dust, which in turn indicates the orientation of the magnetic field.

Models of turbulence

- Historically the first model describing the turbulent phenomenon is due to Kolmogorov (1941). It is a phenomenological model of incompressible homogeneous isotropic (unmagnetized) viscous fluid (described by the Navier-Stokes Eq.). The main results of the Kolmogorov theory are:
  1. The velocity perturbation at a scale ℓ between the injection scale L and dissipation $\ell_{\rm d}$ is only dependent on the the velocity at the injection scale $U_{\rm L}$: $\delta u(\ell) \sim U_{\rm L} \times \left(\frac{\ell}{L}\right)^{1/3}$.
  2. The power 1D spectrum: $E(k) = C_{\rm K} k^{\alpha} \epsilon^{\beta}$, $\alpha = -5/3$ and $\beta = 2/3$ and $C_{\rm K}$ is called the universal Kolmogorov constant, experimentally derived to ~ 1.5.
  3. The dissipation scale is $\ell_{\rm d} = L\mathcal{R}^{-3/4}$, where $\mathcal{R}$ is the Reynolds number $U_{\rm L}L/\nu$, ν is the kinetic viscosity.
- However the ISM is compressible (the sonic Mach number is a few), magnetized ...

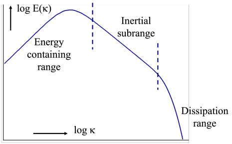

Main form and scales of a turbulent power spectrum.

Homogeneous incompressible magnetized turbulence

With the presence of a magnetic field, the turbulent energy cascades due to interaction of counter propagating wave-packets. They may be anisotropic with perturbation scales $\ell_{||}$ parallel to the background MF and $\ell_{\perp}$ perpendicular to the background MF.
Considering Alfvénic perturbations we have two main timescales $\tau_{||} = (k_{||} u_A)^{-1}$, the crossing time of two packets, and $\tau_{\ell} = (k_{\perp} \delta u_{\ell})^{-1}$ the shearing time of two wave packets. Different phenomenology exists depending on the geometry and the strength of the turbulence 1) weak interaction $\tau_s \gg \tau_A$ 2) strong interaction $\tau_s \ll \tau_A$.

1. Kraichnan phenomenology (Kraichnan 1965): The turbulence is isotropic and weak, the 1D spectrum scales as $E(k) \propto k^{-3/2}$.
2. Weak anisotropic MHD turbulence (Galtier-Nazarenko, Galtier et al 2000) phenomenology, the spectrum scales as $E(k) \propto k_{\perp}^{-2}$.
3. Goldreich-Sridhar phenomenology (Goldreich-Sridhar 1995). The turbulence is anisotropic and strong. The anisotropy is fixed by the critical balance which stipulates $\tau_s = \tau_A$ which leads to $k_{||} = k_{\perp}^{2/3} L^{-1/3}$. The 1D spectrum $E(k) \propto k_{\perp}^{-5/3}$.

Notice that more complex phenomenology do exist, eg a purely 3D one proposed by Boldyrev (2005).

A bit more on the Goldreich-Sridhar model

This model is characterized by a scale-dependent geometry.

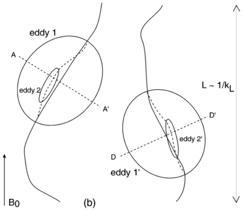

Two Goldreich-Sridhar Eddies at two different scales, from Cho et al 2002.

The 3D spectrum can be written as:

$$E(\vec{k}) \propto k_\perp^{-10/3} G(u) \ , \ u = k_\| L/(k_\perp L)^{2/3} \ , \tag{34}$$

we have some freedom in the choice of the function G(u) such that $\int_0^\infty G(u) du = 1$ and $G(u) \to 0$ as $u \to \infty$. Chandran (2000) G = Heaviside function, Cho et al (2002) G= exponential function. The exact choice has some impact, see eg anistropy studies below.

Homogeneous compressible magnetized turbulence

- In compressible case now **three** MHD modes are involved: Alfvén modes, fast and slow-magnetosonic modes (see section on MHD waves in lecture 1).
- (remind) The behavior of these modes depends on the plasma beta parameter = gas pressure/magnetic pressure.

$$\beta_{\rm p} = \frac{8\pi nkT}{B^2} \simeq 0.45 \frac{n}{0.1\ {\rm cm}^3} \frac{T}{1{\rm eV}} \left(\frac{B}{3\mu{\rm Gauss}}\right)^{-2} \tag{35}$$

  In the ISM $\beta_{\rm p}$ is typically in the interval 0.1-10.
- No phenomenology exist, we have to rely on numerical simulations.

$\rightarrow$ an useful tool: the structure function of order n, for a quantity f.

$$S_n = \langle (f(\vec{x}_1) - f(\vec{x}_2))^n \rangle \tag{36}$$

MHD numerical simulations results

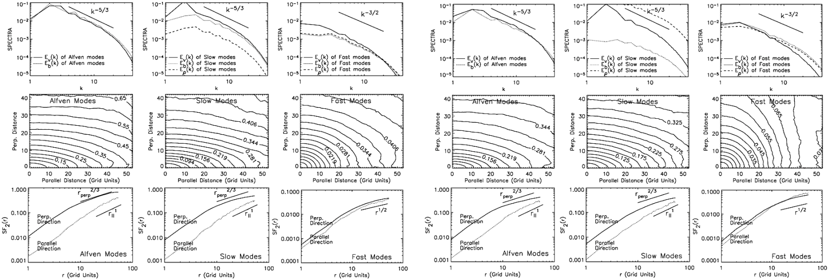

Spectrum, anisotropy and structure function for Alfvén, slow and fast magnetosonic modes (Cho & Lazarian 2003).

Left $\beta_p = 4, M_s = 2.3$, right $\beta_p = 0.2, M_s = 0.35$

→ Alfvén and slow magnetosonic turbulence are anisotropic and follow the Goldreich-Sridhar scaling while fast magneto sonic turbulence is isotropic and follows the Kraichnan scaling.

Super-Alfvénic turbulence

Super-Alfvénic turbulence occurs when $M_a = U_L/u_A > 1$.

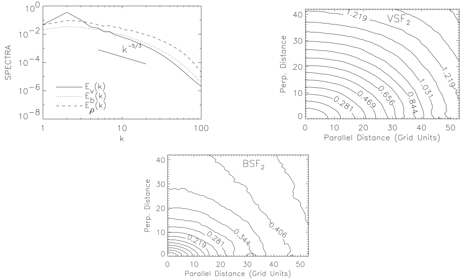

Spectrum, velocity and magnetic structure function of Alfvénic turbulence, $M_A = 8$, $M_s = 2.5$, (Cho & Lazarian 2003)

It can be seen a transition from isotropy to anisotropy below a scale $L_A = L/M_a^3$. At small scales the GS scaling is recovered. Above, the turbulence is isotropic, Kolmogorov like.

Magnetic field structure in the Galaxy

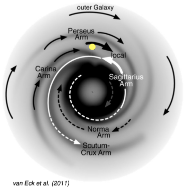

Model of the large scale magnetic field in the Galaxy (court. K. Ferrière)

The magnetic field structure in our Galaxy is twofolds (Ferrière 2001). It can be obtained from different observational techniques: Faraday rotation, synchrotron radiation, dust polarization, Zeeman effect.

- Regular components, they vary from different locations.
  - Nearby the solar system (local ISM) $B_{\rm reg} \sim 1.5\ \mu G$
  - In the galactic disk, it varies if we consider arm/inter-arm regions $B_{\rm reg} \sim 1 - 5\ \mu G$
  - In the halo $B_{\rm reg,z} \sim 0.3\ \mu G$.
- Random components:
  - Nearby the solar system (local ISM) $B_{\rm rms} \sim 5\ \mu G$
  - In the galactic disk, it varies also $B_{\rm rms} \sim 6\ \mu G$

More on the turbulent component: The power-spectrum

Faraday rotation measurements give two informations: 1) the rotation measure $RM = \int_0^D n_e B_{||} ds$ 2) the emission measure $EM = \int_0^D n_e^2 ds$, where n_e is the thermal electron density along the line of sight (LOS), and $B_{||}$ is the MF along the LOS, D is the distance through the medium to the source.

The RM and EM structure function of order 2 $D_{RM} = \langle (RM(\theta) - RM(\theta + \delta\theta))^2 \rangle$ (the same for EM) give:

$$D_{RM}, D_{EM} \propto \begin{cases} \delta\theta^{5/3} & \text{for } \theta \leq 0.07^o, \quad (37) \\ \delta\theta^{2/3} & \text{for } \theta > 0.07^o, \quad (38) \end{cases}$$

which translates into

$$E_n, E_B \propto \begin{cases} k^{-5/3} & \text{for } \ell \leq 3.6\text{pc}, \quad (39) \\ k^{-2/3} & \text{for } \ell > 3.6\text{pc}. \quad (40) \end{cases}$$

Transition from 2D to 3D Kolmogorov turbulence around 4 pc.

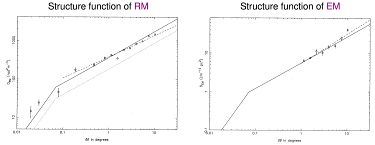

The structure function SF2 of the turbulent component obtained from DM, EM measurements in ionized media (Minter & Spangler 1996), D=2.9 kpc.

The turbulence outer scale

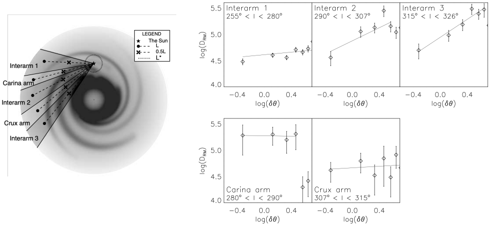

Arm/inter-arm DM structure function (Haverkorn et al 2008).

- In inter-arm regions, typical outer scale $\sim$ 100pc, Kolmogorov below a few pc.
- In spiral arm regions, outer scales a few pc, Kolmogorov below a few pc, reduced flat part.

Traces a stronger stellar activity (winds, Supernova explosions ...) in spiral arms.

Outlines

Observations: large scale anisotropy (LSA)

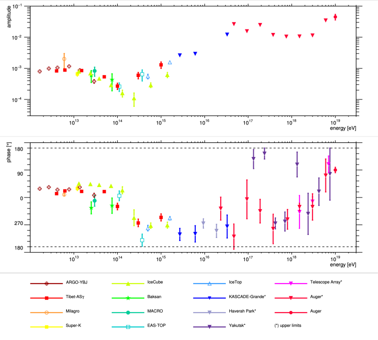

Dipole anisotropy amplitude and phase as function of CR energy (Deligny 2018).

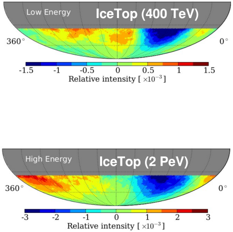

Large scale anisotropy as seen by the Icetop experiments (Aartsen et al 2013).

Observations: small scale anisotropy (SSA)

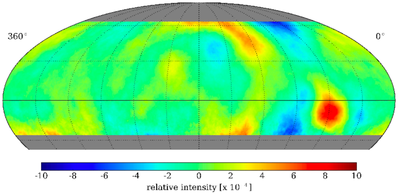

Small scale anisotropy as observed by HAWC collaboration at 2 TeV (Abeysekara et al 2014).

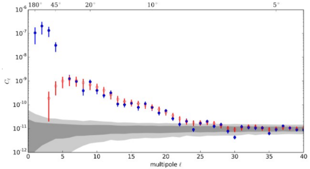

Small scale anisotropy multlipole development (blue Icetop at 20 TeV, red HAWC at 2 TeV).

CR dipole

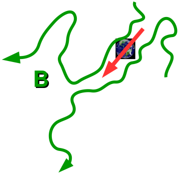

Sketch of the CR dipole along the local MF lines (court. G. Giacinti) .

CR dipole direction is compatible with the local magnetic field direction (IBEX observations, Schwardon et al 2014). This can be interpreted as CR mostly diffusing along the local field line (Giacinti & Kirk 2017).

The amplitude of the dipole is

$$\delta = \frac{3\kappa_{\parallel}}{c} \frac{|\vec{\nabla} n_{\rm CR}|}{n_{\rm CR}} . \tag{41}$$

So the amplitude of LS anisotropy provides a constrain on $\kappa_{\parallel}$ and hence on $D_{\mu\mu}$ (see Eq. 15). So different models of CR scattering can be tested once we can derive $D_{\mu\mu}$ (Giacinti & Kirk 2017).

$$D_{\mu\mu} \propto \sum_{n=-1}^{1} \int d^3\vec{k} \times \left(\frac{n^2 J_n^2(w)}{w^2} W_{\rm A}(\vec{k}) + \frac{k^2 J_n'^2(w)}{w^2} W_{\rm S/F}(\vec{k}) \right) R(\vec{k}), \tag{42}$$

with $w = k_{\perp} r_{\rm L}$.

Constraining the local magnetized turbulence

Giacinti & Kirk (2017) have tested two types of models and two types of resonance function.

1. Goldreich-Sridhar turbulence (for Alfvén, slow magnetosonic modes, see slide 53) with two types of spectrum either by Chandran (2000) [Heaviside function] or Cho et al (2002) [exponential].
2. Resonance function: either Dirac (QLT), or one obtained from resonance broadening (see Eq. 31).

Main results: Some models can be rejected, eg scattering by FM turbulence with Dirac Resonance condition. GS models fit the LS anisotropy data.

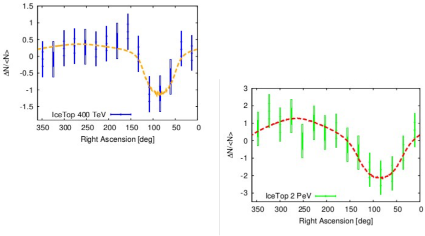

Fit of the CR LS anisotropy, RA profile with GS model (exponential, broad resonance) (court. G. Giacinti)

Outlines

ISM phases

Ideally the ISM can be cast into different thermal phases (stable solutions of the thermal instability) in rough pressure equilibrium each other (P/k_B is the same), see Jean et al 2009.

Hot phase or hot ionized gas phase : HISM = temperature T=10^6 K, mean total density n=$10^{-3} - 10^{-2}$ cm^{-3}, volume filling factor $f \sim 0.5$, ionization fraction $x = 1$.

Warm ionized phase : WIM = T $\simeq$ 8000 K, n=0.2-0.5 cm^{-3}, $f \sim 0.3$, $x \simeq 0.9$.

Warm neutral or atomic phase : WNM = T=6000-10000 K, n=0.2-0.5 cm^{-3}, $f \sim 0.3$, $x \simeq 0.1$.

Cold neutral or atomic phase : CNM = T=50-100 K, n=20-50 cm^{-3}, $f \sim 0.01$, $x \simeq 10^{-3}$.

Molecular phase or clouds : MCs = T=10-20 K, n=$10^2 - 10^6$cm^{-3}, $f < 0.01$, $x = 10^{-4} - 10^{-6}$.

Wave damping processes

Two types of damping process: collisionless (through the interplay of electromagnetic fields) or collisional (through collisions between species). Collisionless (Collisional) damping of a perturbation of wavelength λ dominates if the proton thermal mean free path $\ell_{\rm th,p} > \lambda$ ($\ell_{\rm th,p} < \lambda$), see Yan & Lazarian (2004), where for a medium of density n and temperature T we have:

$$\ell_{\rm th,p} = v_{\rm th} t_{\rm coll} \simeq 6\ 10^{11}\ {\rm cm} \left(\frac{\rm T}{8000\ {\rm K}}\right) \left(\frac{\rm n}{1\ {\rm cm}^{-3}}\right)^{-1} . \quad (43)$$

A short list of damping processes.

1. Collisionless: 1) Linear Landau damping, 2) Non-linear Landau damping, 3) Turbulent "damping" (Lazarian 2016) for CR self-generated waves (see next)
2. Collisional: 1) ion-neutral collisions 2) viscous damping ...

We have to compare for each ISM phase $\ell_{\rm th,p}$ with the turbulent wavelength at the injection scale L= 100-50 pc (Yan & Lazarian 2004, table 1):

THE PARAMETERS OF IDEALIZED ISM PHASES AND RELEVANT DAMPING

Parameter	Galactic Halo	HIM	WIM	WNM	CNM	DC
T (K)	2×10^6	1×10^6	8000	6000	100	15
C_S (km s^{-1})	130	91	8.1	7	0.91	0.35
n (cm^{-3})	10^{-3}	4×10^{-3}	0.1	0.4	30	200
$l_{\rm mfp}$ (cm)	4×10^{19}	2×10^{18}	6×10^{12}	8×10^{11}	3×10^6	10^4
L (pc)	100	100	50	50	50	50
B (μG)	5	2	5	5	5	15
β	0.28	3.5	0.11	0.33	0.42	0.046
Damping	Collisionless	Collisional	Collisional	Neutral-ion	Neutral-ion	Neutral-ion

Impact over CR propagation

The damping process fixes a minimum scale k_c^{-1} of the turbulence spectrum such that $\Gamma_d \tau_{casc} = 1$, Γ_d is the damping rate and τ_{casc} is the Eddy turnover cascade time, e.g. $\tau_{casc}^{-1} = k\delta u_\ell \sim \frac{U_L}{L}\left(\frac{L}{\ell}\right)^{2/3}$ in Kolmogorov phenomenology.

Hence the cut-off is inserted into the calculation of 1) the power spectrum (e.g.) $\delta B^2 = \int_{k_c}^{k_{min}} d^3\vec{k} W(\vec{k})$ 2) diffusion coefficients (e.g. in the case of Alfvénic turbulence)

$$D_{\mu\mu} \propto \sum_{n=-1}^{1} \int_{k_c}^{k_{min}} d^3\vec{k} \left(\frac{n^2 J_n^2(w)}{w^2}\right) W_A(\vec{k}) R(\vec{k}).$$

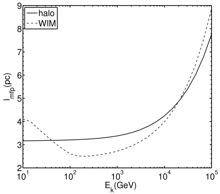

CR mfp in the WIM and halo phases. The effect of collisional damping at small scales can be seen in the WIM, the mfp increases below 100 GeV (from Yan & Lazarian (2008).

Propagation in a multi-phase ISM in large-scale-injected turbulence

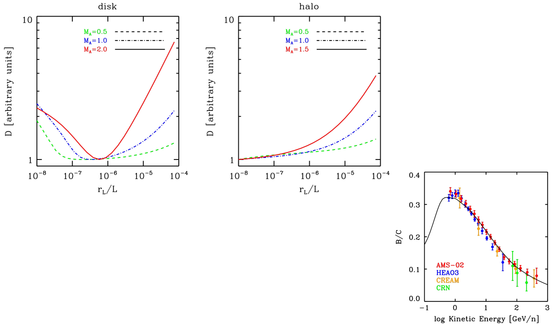

CR mfp for two distinct galactic locations and for different Alfvénic numbers (from Evoli & Yan (2014)). Fit of CR including a spectral break around 100 GeV for the model $M_A = 2$ in the disk and $M_A = 1$ in the halo.

An example of modeling considering a disk + a halo, the mfp is calculated using resonance broadening and Alfvénic and FM turbulence (Evoli & Yan 2014). The break is produced by the effect of the collisional damping in the disk.

Outlines

CR induced instabilities

CR are an important source of free energy, they can induce instabilities through very different ways (Bykov et al 2013).

- Anisotropic particle distribution : resonant streaming instability (Skilling 1975), gyroresonance instability (Lazarian & Beresnyak 2006).
- Current-driven instability : non-resonant streaming instability (Gary 1993, Bell 2004).
- Pressure-driven instabilities : firehose, mirror-type (Blandford & Funk 2007)
- Pressure gradient driven instability (Drury & Falle 1986).

$\rightarrow$ Below we concentrate on the resonant and non-resonant regimes of the streaming instability. The non-resonant instability results from the Lorentz force $\vec{J}_{\rm CR}/c \wedge \vec{B}$ imposed by the CR current and the resonant instability results from an anisotropic CR population with a distribution elongated along the background MF. In both cases the background plasma will back-reaction by trigering either a counter-balancing current or by supporting Alfvén waves extracting momentum to the CRs.

The streaming instability I

Growth rate derivation in the cold plasma limit (Krall & Trivelpiece 1973, Zweibel 2003, Amato & Blasi 2009, Bykov 2013), in hot plasmas (Achterberg 1981).
Krall & Trivelpiece give the first order perturbation electric field in the case of uniformly magnetized plasma from the perturbation analysis of the Vlasov Eq.

$$-\vec{k} \wedge \vec{k} \wedge \delta\vec{E} = \frac{\omega^2}{c^2}\delta\vec{E} + i\frac{\omega}{c^2}\sum_\alpha n_\alpha q_\alpha \int d^3\vec{v}\vec{v}\delta f_{\alpha,\mathrm{k}} \ . \tag{44}$$

α stands for the different species in the problem (thermal ions/electrons, non-thermal ions/electrons) and the perturbed distribution is $\delta f_\alpha(\vec{x},\vec{v},t) = \delta f_{\alpha,\mathrm{k}} \exp\left(i(\vec{k}.\vec{x} - \omega t)\right)$, it can be expressed in terms of ordinary Bessel functions. The dispersion relation results from the determinant calculation of a 3x3 matrix.

We restrict the analysis to circularly polarized waves propagating parallel to the background MF (less subject to damping). Following Zweibel (2003) we consider a population of cold background electron and protons and a population of CR (mostly) drifting wrt to the background plasma at a speed u_{D}.

The streaming instability II

The relation dispersion in the thermal plasma frame then reads (Zweibel 2003):

$$\omega^2 + \omega_{\rm cp} \frac{n_{\rm CR}}{n_{\rm th,i}} \left(\omega - k u_{\rm D}\right) \zeta(k) - k^2 u_{\rm A}^2 = 0 \;, \qquad (45)$$

where the effect of CR is hidden in $\zeta(k)$, it modifies the Alfvén wave dispersion.

- Non-resonant modes have a maximum growth rate $\Gamma_{\rm max} = \sqrt{k\sigma/R_{\rm g}}$, important at fast shocks (see L. Drury lectures).
- Resonant modes have a maximum growth rate $\Gamma_{\rm max} = \sqrt{\pi\sigma/R_{\rm g}k}$

$$\sigma = u_{\rm A}^2 \frac{4\pi J_{\rm CR}}{c} \frac{R_{\rm g}}{B} .$$

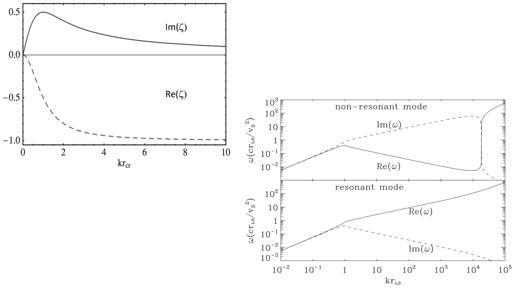

Left: function ζ as function of $kr_{\rm g}$ (Zweibel 2003). Right: Re and Im partis of the frequency for right-handed non-resonant (up) and left-handed resonant (down) streaming modes as function of $kr_{\rm g}$ (Amato & Blasi 2009). The growth rate of the NR mode scales as $\sqrt{k}$, the growth rate of the resonant mode scales k. The CR distribution is taken to be $f(p) \propto p^{-4}$.

The resonant streaming instability

We recast the resonant streaming instability growth rate following the procedure adopted in Skilling (1971, 1975). The anisotropy of the particle distribution δf is controlled by the space-energy dependence of the isotropic zero$^{\rm th}$ order distribution $f(\vec{x}, v, t)$:

$$\nu(\mu)_\pm \frac{\partial \delta f}{\partial \mu} = -v \frac{\vec{B}}{B} . \vec{\nabla} f + \nu_\pm \vec{w}_\pm . \frac{\vec{B}}{B} \frac{p}{v} \frac{\partial f}{\partial p} \ , \tag{46}$$

where $\nu_\pm$ is the angular scattering frequency by forward (+)/backward(-) propagating waves and $\vec{w} = \vec{u} \pm \vec{u}_{\rm A}$ is the forward/backward wave propagation speed with respect to the background plasma.
If only forward waves are generated then the growth rate is

$$\Gamma_{\rm g}(k) = -\frac{4\pi}{3} \frac{p^4 u_{\rm A}}{W(k) k} v \frac{\vec{B}}{B} . \vec{\nabla} f|_{p=qB/kc} \ , \tag{47}$$

so proportional to the gradient of CR along the background MF, it is a growth only along a negative gradient. The condition is verified for resonant waves with $k r_{\rm g} = 1$.

Quasi-linear theory of self-generated turbulence

Within the QLT framework we write a couple system of equations coupling the CR distribution function f and the wave energy density $W(k)$ (Blasi et al 2012). In 1D (the height above the disk z), the stationary system reads:

$$u_A \frac{\partial f}{\partial z} - \frac{du_A}{dz}\frac{p}{3}\frac{\partial f}{\partial p} = \frac{\partial}{\partial z}\left(\kappa \frac{\partial f}{\partial z}\right) + Q_{CR} \ , \ \kappa = \frac{r_g v}{3kW(k)} \ , \tag{48}$$

$$\Gamma_{growth} - \Gamma_d = Q_W . \tag{49}$$

We have added two terms Q_{CR} and Q_W for CR and wave sources. The damping process adopted here has a cascade form $\Gamma_d = -\partial_k \kappa_{kk} \partial_k W(k)$ with $\kappa_{kk} \propto k^{7/2}\sqrt{W(k)}$. The growth rate is given by Eq. 47. In that case
$f(z) = f(z=0)\,(1 - \exp(-u_A H/\kappa(1-|z|/H))/(1-\exp(-u_A H/\kappa)))$. H is the scale height of the halo. The two above Eqs. are solved iteratively to deduce the particle and wave spectrum in the disk with the assumption that both κ and u_A are weakly dependent on z.

Energy-dependent regimes

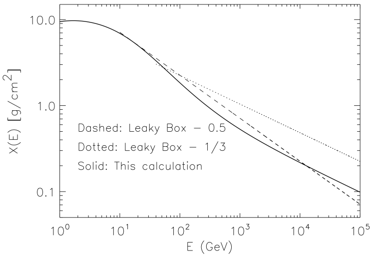

Grammage calculated using the QLT model of Blasi et al (2012) compared with two leaky-box solutions (see D. Maurin lectures) for two different escape time energy dependence.

A spectral hardening occurs –naturally – around 200 GeV for standard values of the galaxy radius, halo size, energy in Supernova and the fraction of it imparted into CRs.

Outlines

Observations: halos around pulsars

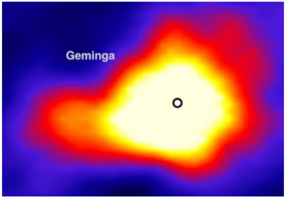

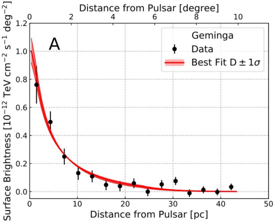

Gamma-ray (8-40 TeV) halos around the Geminga pulsar, by 100 TeV electrons. Model of the emission radial profile (diffusive, loss Eq.), HAWC collaboration (2017).

The radial gamma-ray profile is best reproduced with $\kappa \sim 4.5\ 10^{27}\ \mathrm{cm}^2/\mathrm{s}$, thus about two orders of magnitude below "standard" estimates deduced from S/P ratios.

Modelling: halos around pulsars

- Evoli et al (2018). Lepton-induced self-generated turbulence through a streaming instability.
- Fang et al (2019). Turbulence generated at the SNR shock wave. The pulsar is still inside.
- Lopez-Coto & Giacinti (2018). Diffusion in isotropic 3D turbulence. The diffusion coefficient value constrains the coherence scale to be pc and the MF to be completely disordered with strength $B_{\rm rms} \sim 3\ \mu$G.

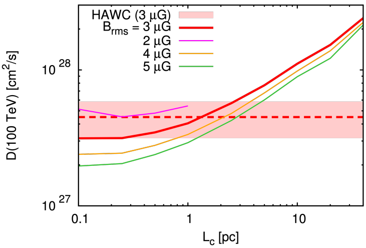

Diffusion coefficient of CR leptons in isotropic 3D Kolmogorov turbulence for different coherence lengths ℓ_c and different values of the turbulent MF (Lopez-Coto & Giacinti 2018).

Observations: halos (?) around supernova remnants

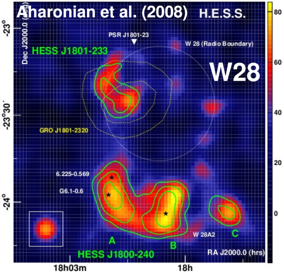

Gamma-ray emission by molecular clouds (A,B, C) around the SNR W28 (Aharonian et al 2008).

Solving a diffusion Eq. Gabici et al (2007) find a diffusion coefficient reduced by a factor $\sim$ 16.

A model of CR halo: the CR cloud model: Malkov et al 2013

Main assumptions:

- Particle acceleration at polar cusps, more efficient if the magnetic field is parallel to the shock normal (see L.Drury lectures).
- 1D propagation over distances below the background MF coherence length ℓ_c, of the order of 100 pc.
- Injection of a given SNR power into CRs.
- Solving a couple system of Eqs for CR pressure P_{CR} and self-generated waves energy density $I(k) = kW(k)$.

$$\frac{\partial P_{\rm CR}}{\partial t} + u_{\rm A}\frac{\partial P_{\rm CR}}{\partial z} = \frac{\partial}{\partial z}\left(\kappa \frac{\partial P_{\rm CR}}{\partial z}\right) , \qquad (50)$$

$$\frac{\partial I}{\partial t} + u_{\rm A}\frac{\partial I}{\partial z} = 2\left(\Gamma_{\rm growth} - \Gamma_{\rm d}\right) I + Q_{\rm I}. \qquad (51)$$

Where the diffusion coefficient $\kappa = \frac{r_{\rm g} c}{I(k)}$ and $\Gamma_{\rm growth}$ is the growth rate of resonant ($kr_{\rm g}$=1) modes, $\Gamma_{\rm d}$ is the damping rate, $Q_{\rm I}$ is the background turbulence level.

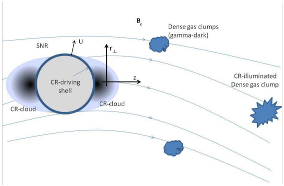

Sketch of the Cosmic Ray Cloud model (Malkov et al 2013).

A phase-dependent CRC model

The main effect is due to the wave damping term Γ_d. Here a couple of examples of its value in different ISM phases. In partially ionized phases ion-neutral collisions dominate wave damping.

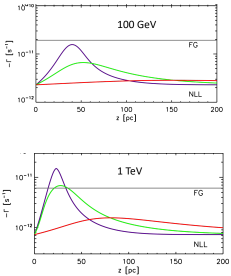

Damping rate in the HISM

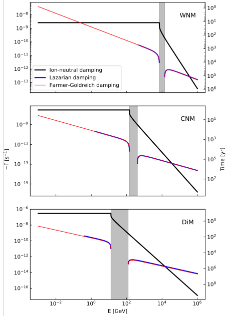

Damping rate in the HISM at two energies (Nava et al 2019) and in the partially ionized phases (Brahimi et al 2019). NLL= non-linear Landau damping, FG= Farmer-Goldreich damping (damping in the background turbulence, Farmer & Goldreich (2004)), turbulent or Lazarian damping (Lazarian 2016).

Solutions in the HISM

Solutions in the HISM phase

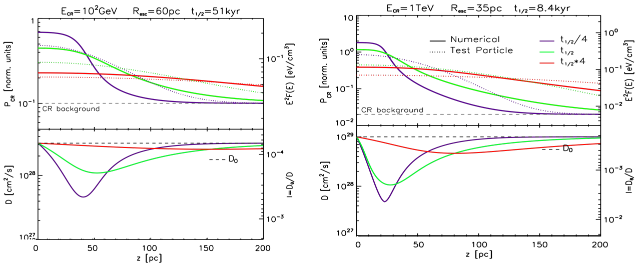

Test-particle= solutions in the background diffusion coefficient (the one deduced from S/P ratios), Numerical=solving Eqs. 50, and 51, Nava et al (2019).

Solutions in the partially ionzed phases

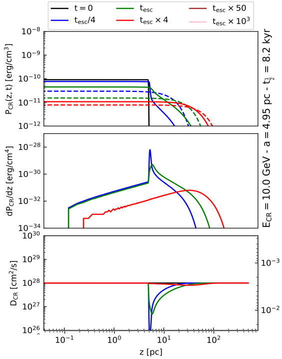

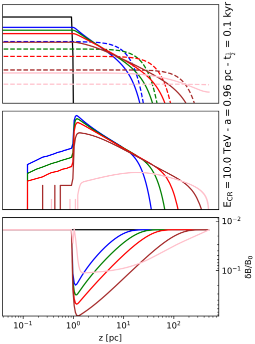

CR propagation in the CNM phase (Brahimi et al 2019).

Outlines

Perspectives

- Several recent observations provide tighter constraints on CR propagation in the ISM: Anisotropy (small/large scale), spectral breaks.
  - Anisotropy constrains local ISM propagation as well as heliosphere-ISM interaction.
  - Spectral breaks give a hint that 1-100 GeV CRs are able to produce their own turbulence.
- Detection of gamma-ray halos around Pulsars and some hints of CR propagation around supernova remnants: impact of sources.
- Extend to the role of CR sources (SNR, pulsars, Super-bubbles) in ISM dynamics, star formation: launching galactic winds, interaction with molecular clouds (ionization/heating, see M. Padovani lectures), CR acceleration in young stars ...

Outlines

- M.G. Aartsen et al, 2013, Observation of Cosmic-Ray Anisotropy with the IceTop Air Shower Array, ApJ, 765, 55.
- A.U. Abeysekara et al, 2014, Observation of Small-scale Anisotropy in the Arrival Direction Distribution of TeV Cosmic Rays with HAWC, ApJ, 796, 108.
- A.U. Abeysekara et al, 2017, Extended gamma-ray sources around pulsars constrain the origin of the positron flux at Earth, Science, 358, 911.
- A. Achterberg, 1981, On the propagation of relativistic particles in a high beta plasma, A&A, 98, 161.
- F. Aharonian et al, 2008, Discovery of very high energy gamma-ray emission coincident with molecular clouds in the W 28 (G6.4-0.1) field, A&A, 481, 401.
- E. Amato & P. Blasi, 2009, A kinetic approach to cosmic-ray-induced streaming instability at supernova shocks, MNRAS, 392, 1591.
- A.R. Bell, 2004, Turbulent amplification of magnetic field and diffusive shock acceleration of cosmic rays, MNRAS, 353, 550.
- P. Blasi, E. Amato, P. Serpico, Spectral Breaks as a Signature of Cosmic Ray Induced Turbulence in the Galaxy, PRL, 109, 1101.
- R.D. Blandford & S. Funk, 2007, he Magnetic Bootstrap,n The First GLAST Symposium, AIP Conference, Series, Vol. 921 (2007), pp. 624.
- S. Boldyrev, 2006, Spectrum of Magnetohydrodynamic Turbulence, Physical Review Letters, 96, 115002.
- L. Brahimi, A. Marcowith, V.S. Ptuskin, Non-linear Diffusion of Cosmic Rays Escaping from Supernovae Remants in the Cold Partially Neutral Atomic and Molecular Phases, arXiv:1909.04530.
- A. Bykov et al, 2013, Microphysics of Cosmic Ray Driven Plasma Instabilities, SSRv, 178, 201.
- B.D.G. Chandran, 2000, Scattering of Energetic Particles by Anisotropic Magnetohydrodynamic Turbulence with a Goldreich-Sridhar Power Spectrum, Physical Review Letters, 85, 4656.
- J. Cho & A. Lazarian, 2003, Compressible magnetohydrodynamic turbulence: mode coupling, scaling relations, anisotropy, viscosity-damped regime and astrophysical implications, MNRAS, 345, 325.
- L.O.'C. Drury & S. A. E. G. Falle, On the Stability of Shocks Modified by Particle Acceleration, MNRAS, 223, 353.
- C. Evoli & H. Yan, 2014, Cosmic Ray Propagation in Galactic Turbulence, ApJ, 782, 36.
- C. Evoli, T. Linden, G. Morlino, 2018, Self-generated cosmic-ray confinement in TeV halos: Implications for TeV ? -ray emission and the positron excess, PRD, 98, 063017.
- K. Fang, X.J. Bi, P.-F. Yen, Reanalysis of the Pulsar Scenario to Explain the Cosmic Positron Excess Considering the Recent Developments, ApJ, 884, 124.

- A. Farmer & P. Goldreich, 2004, Wave Damping by Magnetohydrodynamic Turbulence and Its Effect on Cosmic-Ray Propagation in the Interstellar Medium, ApJ, 604, 671.
- K.M. Ferrière, 2001, The interstellar environment of our galaxy, RMPhys, 73, 1031.
- S. Galtier et al, 2000, A weak turbulence theory for incompressible magnetohydrodynamics, Journal of Plasma Physics, 63, 488.
- S. Gary, 1993, Theory of space plasma microinstabilities, Cambridge.
- G. Giacinti & J.G. Kirk, 2017, Large-scale Cosmic-Ray Anisotropy as a Probe of Interstellar Turbulence, ApJ, 835, 258.
- P. Goldreich & S. Sridhar, 1995, Toward a Theory of Interstellar Turbulence. II. Strong Alfvenic Turbulence, ApJ, 438, 763.
- M. Haverkorn et al, 2008, The Outer Scale of Turbulence in the Magnetoionized Galactic Interstellar Medium, ApJ, 680, 362.
- P. Jean et al, 2009, Positron transport in the interstellar medium, A&A, 508, 1099.
- A. N. Kolmogorov, 1941 Dissipation of energy in locally isotropic turbulence, C. R. Acad. Sci. U.S.S.R, 32:168.
- A. Krall & A W. Trivelpiece, 1973, Principles of plasma physics, McGraw-Hill.
- R. Lopez-Coto & G. Giacinti, 2018, Constraining the properties of the magnetic turbulence in the Geminga region using HAWC ?-ray data , MNRAS, 479, 4526.
- A. Lazarian & A. Beresnyak, 2006, Cosmic ray scattering in compressible turbulence, MNRAS, 373, 1195.
- M.A. Malkov et al, 2013, Analytic Solution for Self-regulated Collective Escape of Cosmic Rays from Their Acceleration Sites, ApJ, 768, 73.
- Minter A. H. & Spangler S. R., 1996, Observation of Turbulent Fluctuations in the Interstellar Plasma Density and Magnetic Field on Spatial Scales of 0.01 to 100 Parsecs, ApJ, 458, 194.
- L. Nava et al, 2019, Non-linear diffusion of cosmic rays escaping from supernova remnants - II. Hot ionized media, MNRAS, 484, 2684.
- N. Schwadron et al, 2014, Global Anisotropies in TeV Cosmic Rays Related to the Sun Local Galactic Environment from IBEX, Science, 343, 988.
- J. Skilling, 1971, Cosmic Rays in the Galaxy: Convection or Diffusion?, MNRAS, 170, 265.
- J. Skilling, 1975, Cosmic ray streaming - I. Effect of Alfvn waves on particles, MNRAS, 172, 557.
- E. Zweibel, 2003, Cosmic-Ray History and Its Implications for Galactic Magnetic Fields, ApJ, 587, 625.

Final words

Thank to the organizers for the invitation,

Thank you all for your attention.